

Phase analysis of gated blood pool SPECT for multiple stress testing assessments of ventricular mechanical dyssynchrony in a tachycardia-induced dilated cardiomyopathy canine model

Samaneh Salimian, MSc,^a Bernard Thibault, MD,^b Vincent Finnerty, MSc,^a Jean Grégoire, MD,^a and François Harel, MD, PhD^a

^a Department of Nuclear Medicine, Montreal Heart Institute and University of Montreal, Montreal, QC, Canada

^b Department of Medicine, Montreal Heart Institute and University of Montreal, Montreal, QC, Canada

Received Jun 12, 2015; accepted Nov 6, 2015

doi:10.1007/s12350-015-0338-6

Background. Stress-induced dyssynchrony has been shown to be independently correlated with clinical outcomes in patients with dilated cardiomyopathy (DCM) and narrow QRS complexes. However, the extent to which stress levels affect inter- and intraventricular dyssynchrony parameters remains unknown.

Methods. Ten large dogs were submitted to tachycardia-induced DCM by pacing the right ventricular apex for 3–4 weeks to reach a target ejection fraction (EF) of 35% or less. Stress was then induced in DCM dogs by administering intravenous dobutamine up to a maximum of 20 $\mu\text{g}\cdot\text{kg}^{-1}\cdot\text{min}^{-1}$. Hemodynamic and ventricular dyssynchrony data were analyzed by left ventricular (LV) pressure measurements and gated blood pool SPECT (GBPS) imaging. In order to assess mechanical dyssynchrony in DCM subjects and compare it with that of 8 normal counterparts, we extracted the following data: count-based indices of LV contraction homogeneity index (CHI), entropy and phase standard deviation, and interventricular dyssynchrony index.

Results. A significant LV intraventricular dyssynchrony (CHI: $96.4 \pm 1.3\%$ in control vs $78.6\% \pm 10.9\%$ in DCM subjects) resulted in an intense LV dysfunction in DCM subjects (EF: $49.5\% \pm 8.4\%$ in control vs $22.6\% \pm 6.0\%$ in DCM), compared to control subjects. However, interventricular dyssynchrony did not vary significantly between the two groups. Under stress, DCM subjects showed a significant improvement in ventricular functional parameters at each level (EF: $22.6\% \pm 6.0\%$ at rest vs $48.1\% \pm 5.8\%$ at maximum stress). All intraventricular dyssynchrony indices showed a significant increase in magnitude of synchrony from baseline to stress levels of greater than or equal to 5 $\mu\text{g}\cdot\text{kg}^{-1}\cdot\text{min}^{-1}$ dobutamine. There were individual differences in the magnitude and pattern of change in interventricular dyssynchrony during the various levels of stress.

Conclusions. Based on GBPS analyses, different levels of functional stress, even in close intervals, can have a significant impact on hemodynamic and intraventricular dyssynchrony parameters in a DCM model with narrow QRS complex. (J Nucl Cardiol 2017;24:145–57.)

Reprint requests: François Harel, MD, PhD, Department of Nuclear Medicine, Montreal Heart Institute and University of Montreal, 5000 Belanger Street, Montreal, QC HIT 1C8, Canada; francois_harel@hotmail.com

1071-3581/\$34.00

Copyright © 2015 American Society of Nuclear Cardiology.

Key Words: Ventricular dyssynchrony • gated blood pool SPECT • dobutamine stress • dilated cardiomyopathy with narrow QRS**Abbreviations**

DCM	Dilated cardiomyopathy
GBPS	Gated blood pool SPECT
TAC	Time–activity curve
ROI	Region of interest
CHI	Contraction homogeneity index
SV	Stroke volume

See related editorial, pp. 158–161

INTRODUCTION

Ventricular mechanical dyssynchrony, defined as a timing disparity in ventricular regional contraction, seems to be present in almost all chronic heart failure (HF) patients.¹ Wall motion discoordination is not exclusively caused by electrical conduction delays; regional heterogeneity in myocardial contractility properties can also modify the synchronicity of contraction.^{1,2} The presence of mechanical dyssynchrony with preserved electrical conduction is apparent in a substantial proportion of patients with dilated cardiomyopathy (DCM) and narrow QRS complexes.³

Exercise-induced intraventricular dyssynchrony has been independently correlated with clinical outcomes (combined endpoint of death, heart transplant, or assist device implantation) in patients with idiopathic DCM and narrow QRS complexes.⁴ However, few studies^{4–7} have investigated the effect of stress on mechanical dyssynchrony in such patients and none have examined the range of difference in inter- and intraventricular dyssynchrony parameters when the patients are submitted to various levels of stress. Moreover, the quantification of stress dyssynchrony in those studies has been performed by different echocardiography-based methods. However, an intrinsic property of these methods lies in their limited reproducibility, since they are largely subject dependent, both in the case of image acquisition and analysis.⁸ Also, there is no standardized methodology with accurate and robust parameters for detecting mechanical dyssynchrony using echocardiographic imaging tools.⁹

In comparison with echocardiographic methods, phase analysis of nuclear cardiology modalities such as gated single-photon emission computed tomography (SPECT) myocardial perfusion imaging (GMPS)¹⁰ and gated blood pool SPECT (GBPS)¹¹ has shown a high reproducibility to effectively assess cardiac mechanical dyssynchrony. While both methods have shown a clear

applicability in this field, GBPS has been preferred in some cases since it is based on volume rather than myocardial wall thickness. In addition, it can provide both inter- and intraventricular dyssynchrony data.

Consequently, we used GBPS in our study to investigate the effects of various levels of dobutamine-induced stress on inter- and intraventricular dyssynchrony parameters in an animal model of tachycardia-induced DCM, a well-characterized model of non-ischemic cardiomyopathy in terms of left ventricular (LV) dilation and systolic dysfunction.¹² This study follows our previous work performed on a control cohort.¹³

METHODS**Study Protocol**

Ten large dogs of either gender (mixed races with mean weight of 40.2 ± 4.5 kg) were submitted to tachycardia-induced HF by pacing the right ventricular apex at 240 bpm for 3–4 weeks until the LV ejection fraction (EF) fell below 35%; we selected a moderate to severely reduced EF to assess variations toward upper or lower EF categories. Experiments were initiated within 48 hours of achieving the target LVEF. The protocol was approved by the institutional Research Ethics Board and all procedures followed the Canadian Council on Animal Care.

The animals underwent general anesthesia with isoflurane 1.5% after induction with doses of $5 \text{ mg}\cdot\text{kg}^{-1}$ ketamine and $0.25 \text{ mg}\cdot\text{kg}^{-1}$ diazepam. SaO_2 was monitored using a standard biomedical cardiac monitor (Eagle 4000, Marquette Medical System, Milwaukee, WI, USA). The dogs' bladders were catheterized in order to prevent radioactive urine spills. Venous and arterial accesses were obtained in carotid and femoral arteries as well as jugular and femoral veins. Those vascular accesses were used to install the following devices. First, a Swan-Ganz catheter (931HF75, Edward Life Sciences, Mississauga, ON, Canada) was introduced in a segmental pulmonary artery to measure the cardiac output using a thermodilution method.¹⁴ This was followed by bolus injections of 10 mL of sterile saline cooled at 4°C to increase the signal stability. We used the cardiac monitor to measure cardiac outputs. Second, a pressure catheter was introduced in the right femoral artery in order to acquire systemic arterial pressure signals. Signals were conditioned by a dedicated control unit and acquired by a signal acquisition system. Dobutamine was infused using the venous access in the left leg. Another pressure catheter (Ventricath 507S, 5F, straight tip, Millar, Houston, TX, USA) was installed in the LV via the left carotid artery access. Signals were conditioned (MPVS Ultra 753-2083, Millar), digitized (ITF156, Emka Technologies, Falls Church, VA, USA), and subsequently analyzed with a dedicated software (Iox2, ver. 2.5.1.6, Emka). It has to be mentioned that hemodynamic results were recorded for eight

dogs out of ten because the Millar system was unavailable. Surface ECGs were recorded using a standard 3-lead configuration (Cardiac Trigger Monitor 3000, Ivy Biomedical Systems Inc., Branford, CT, USA).

The GBPS and surface ECGs were acquired at baseline and for each dobutamine-induced stress level of 2.5, 5, 10, and 20 $\mu\text{g}\cdot\text{kg}^{-1}\cdot\text{min}^{-1}$. The acquisition of GBPS was performed after red blood cell labeling using the UltraTag[®]-^{99m}Tc kit. A single dose of radiopharmaceutical of 1223 MBq in average was injected to animals and baseline images were acquired. Cardiac stress was induced by a dobutamine infusion prepared in 500 $\mu\text{g}\cdot\text{mL}^{-1}$ of normal saline solution and continuously infused over average times of 43.5, 28.4, 36.4, and 34.8 minutes while increasing the outflow to reach the predetermined dosage (Figure 1). Because of dobutamine's short half-life of approximately 2.3 minutes, we used continuous infusion to create a stable dobutamine stress effect for acquiring the SPECT images. On average, the total infusion duration was 143.0 minutes, during which a total volume of 415 mL was infused. Immediately after reaching a target dobutamine concentration level, image acquisition was initiated. There were no rest periods during the entire experiment. Cardiac and peripheral hemodynamic data as well as cardiac contraction synchrony data (using GBPS) were recorded at each stress level. The duration of GBPS acquisition was adjusted throughout the day to reach equal count statistics in spite of ^{99m}Tc decay time; average times of 10.8, 13.4, 14.3, and 14.8 minutes, respectively, were used for each dobutamine-induced stress level. Overall, the dobutamine-induced stress effect lasted approximately 208.1 minutes, with the heart rate continuously increasing at each level. Because of humane considerations, we euthanized the dogs at the end of the experiment with the administration of isoflurane 5% and an intravenous overdose of potassium chloride.

GBPS Acquisition and Reconstruction

Data were acquired on a dual head gamma camera with low-energy high-resolution collimators and 64 projections dispatched on a 360° configuration using 64 × 64 matrix. Data acquisition involved 16 frames per cardiac cycle. Transaxial reconstructions were performed with the ramp filtered back projection and subsequently filtered by 8 mm Gaussian filter.

GBPS Data Processing and Dyssynchrony Analysis

Images were manually reoriented into LV short axis sections (Figure 2). Segmentation was performed using an algorithm based on the invariance of the Laplacian previously developed by our group to deliver a dynamic surface of approximately 400 vertices.¹⁵ In summary, simple geometric assumptions were made to separate LV from RV and atria. Two smoothed isosurfaces (LV and RV) were then determined inside both ventricular regions (LV left of the RV, both below the atria). The GBPS images were filtered with a variable cutoff frequency, and Laplacian was computed for each dataset. Profiles were extracted from each Laplacian image

by sampling along 400 vectors perpendicular to each of the ventricular isosurfaces (LV and RV). These profiles were used to find a pivotal point, where values were least variable between filtered datasets. Since this position was resolution independent, it represented a true edge estimation. This surface was then replaced by 3D self-organizing maps (LV and RV) using standard surfaces to get regular sampling over the ventricles. Again 400 profiles normal to these surfaces were analyzed to determine the invariance of the Laplacian for each bin of all 16 temporal bins (Figure 3). Lastly, post-processing was executed on the surfaces to ensure spatial and temporal continuity. After the segmentation, dynamic regions of interest (ROIs) were estimated over both ventricles. The LV ROI was defined as the pixels totally or partially inside the LV plus all pixels under the valvular plane and within 8 mm (2 pixels) of the LV, but all pixels closer to the RV than the LV were excluded (Figure 4). The same approach was applied to define the RV ROI. Time-activity curves (TACs) for the LV and RV were generated using these ROIs (Figure 4). Count-based LVEF and RVEF were measured directly using the TACs. However, in order to measure the stroke volume (SV) in mL, we had to estimate count-based volumes by adjusting the TACs (dividing by the average TAC and multiplying by the average geometric volume, a method previously shown to be well correlated with magnetic resonance imaging volumetric results¹⁶).

A three-harmonic inter-correlation of the RV and LV TACs was used to compute the phase differences between RV and LV (count-based RVLV delay). These results were expressed in degrees and converted to milliseconds to accommodate readers from different specialties (echocardiography, electrocardiography, etc.). It has to be noted that any comparison between RVLV delays measured by GBPS and with other modalities will not be accurate, since the methods for acquiring RVLV delays using various modalities are totally different.

In addition, we extracted TACs for different regions of the LV from the LV ROI. First, the basal slices (where the surface's normal angle to basal direction was less than 45°) were discarded. Then, apical slices were extracted to evaluate the apical TAC separately. The pixels from remaining median slices were split into four regions (anterior, lateral, inferior, and septal) using their angular position in the short axis slice around the LV center (Figure 5). We first estimated Fourier harmonics of each regional TAC to obtain the phase and amplitude of each LV region. In order to compute the LV intraventricular dyssynchrony parameters, a static ROI was used containing the voxels where the LV dynamic ROI was present at least in half of the temporal frames. Three-harmonic Fourier analysis of all voxel TACs and subsequent count-based amplitudes (A) and phases (θ) were acquired within this ROI. In addition to the phase and amplitude, efficiency (E) of contraction of each voxel was also determined, namely, the portion of amplitude in phase with the remainder of the ventricle.¹⁷ In other words, E represents the portion of amplitude in the direction of the mean phase. Thus, E could be calculated as complex harmonic of each voxel TAC ($Ae^{i\theta}$) divided by the mean phase ($\bar{\theta}$), which is the mean angle of all complex harmonics, as follows:

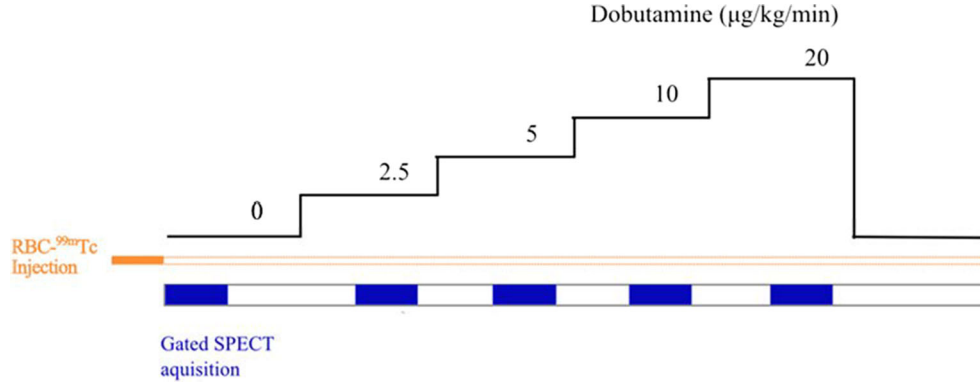


Figure 1. Illustration of dobutamine stress infusion and GBPS acquisition protocol. After injection of a single dose of red blood cells labeled ^{99m}Tc , baseline GBPS images were acquired. Cardiac stress was then induced by a continuous infusion of dobutamine at different levels of 2.5, 5, 10, and 20 $\mu\text{g}\cdot\text{kg}^{-1}\cdot\text{min}^{-1}$. After reaching a stable stress effect at each dobutamine level, GBPS acquisition was performed.

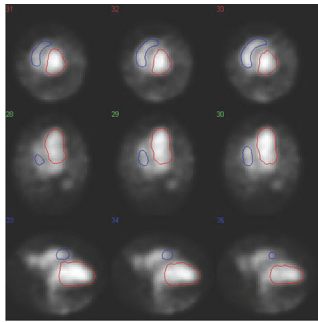


Figure 2. Illustration of GBPS images in short, horizontal, and vertical long axis views, respectively. Regions of interest are drawn over both ventricles. Final 3D segmented *right* (blue) and *left* (red) ventricles derived from those ROIs are shown in the *right* side of the figure.

$$E = \frac{A_1 e^{i\theta_1}}{e^{i\theta}} \quad \bar{\theta} = \overline{\angle A e^{i\theta}}. \quad (1)$$

Based on the above equation, E is actually the projection along the direction of the mean phase in the Fourier space. It would be negative if the voxel phase differed from the mean phase for more than a quarter of the cardiac cycle. In fact, the E index was used to calculate a global contraction homogeneity index (CHI)¹⁷ which was defined as the mean E divided by the mean A . In our point of view, CHI could be interpreted as the proportion of wall movement (endocardial-blood interface movement) that contributes to the stroke volume.

In addition to CHI, phase standard deviation (phase SD) and entropy of the phase histogram were extracted within the LV static ROI. These dyssynchrony parameters have been previously evaluated in planar and radionuclide ventriculography phase analysis.^{11,18,19} Entropy is a degree of randomness of the phase distribution within the ROI. In the case of reduced contraction homogeneity, entropy is able to identify the degree of random and uncoordinated contraction by computing the probability of occurrence of phase angle i (P_i) in a given number of bins (M) of a phase histogram as follows:

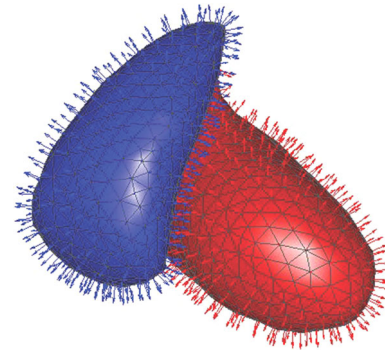


Figure 3. Dynamic surface of approximately 400 vertices over the LV and RV. Vertices are linked together making *triangular shapes* and surface tetrahedrons then are used to estimate the final geometric volumes. Also, 400 profiles normal to the initial surface are shown for both ventricles that are used to estimate the dynamic motion of the surfaces.

$$\text{Entropy} = - \frac{\sum_{i=1}^M P_i \log_2(P_i)}{\log_2(M)}. \quad (2)$$

We used the same equation and method proposed by O'Connell et al to measure the entropy values.¹⁸ It ranges from 0 with complete order to 1 with complete disorder.

Statistical Analysis

Statistical analysis was performed using GraphPad Prism version 6.00 for Windows (GraphPad Software, La Jolla, California, USA). The D'Agostino-Pearson test was used to confirm that the distribution of the hemodynamic as well as dyssynchrony variables was not significantly different from a normal distribution at different dobutamine levels.

Comparisons between rest and dobutamine-induced stress levels for functional and dyssynchrony parameters were made using ANOVA test for repeated measures with Tukey post-test.

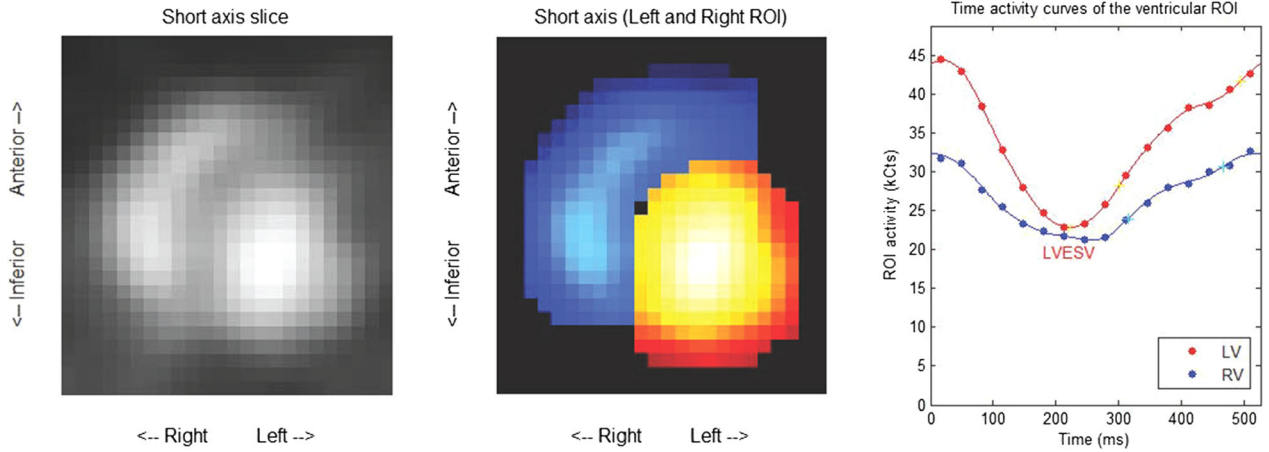


Figure 4. Left and right regions of interest in short axis view and related time–activity curves in 16 bins.

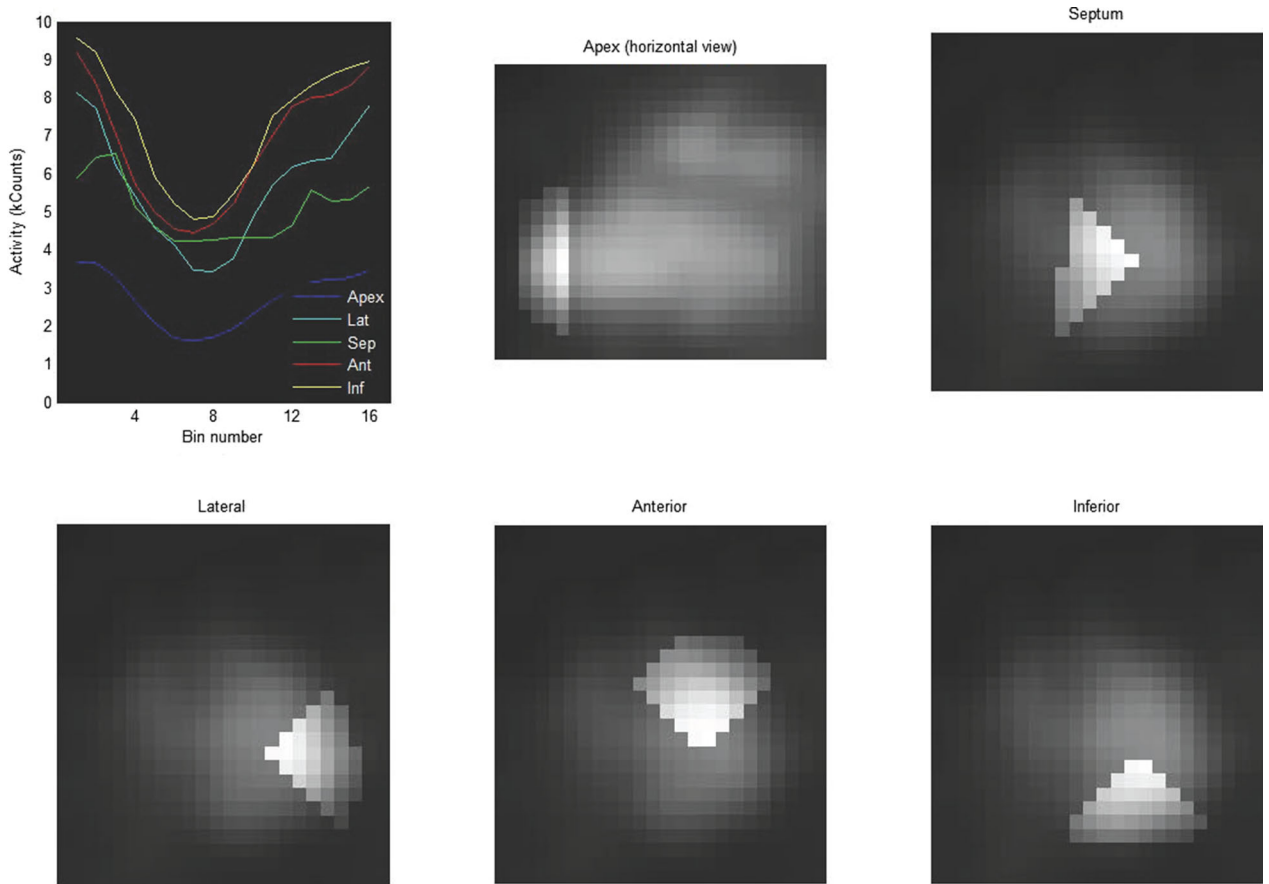


Figure 5. Illustration of time–activity curves for different regions of the LV as well as regional LV ROIs: anterior, lateral, inferior, and septal regions in short axis and apex in horizontal long axis view.

Also, comparisons between control and DCM groups were made using the unpaired Student *t* test. In addition, a correlation test was used to assess the relation between various

cardiac output measurements. Statistical significance was defined as a two-tailed *P* value < .05. Data are shown as mean values ± SD for the continuous variables.

Table 1. Functional parameters at rest and during levels of dobutamine-induced stress in DCM dogs

Index	Dobutamine ($\mu\text{g}\cdot\text{kg}^{-1}\cdot\text{min}^{-1}$)				
	0	2.5	5	10	20
HR (bpm)	107.1 ± 10.5	112.7 ± 12.2	117.8 ± 12.4* [#]	125.7 ± 11.7* ^{##}	134.7 ± 12.2* ^{###} ¶
QRS interval (ms)	79.1 ± 10.2	80.4 ± 9.7	79.5 ± 9.5	78.1 ± 8.7	78.2 ± 7.7
LVEDP (mmHg)	16.9 ± 5.5	16.8 ± 8.5	16.5 ± 8.5	13.7 ± 9.1	16.1 ± 10.7
dP/dt _{max} (mmHg·s ⁻¹)	949.5 ± 238.5	1343.2 ± 277.3*	1660.5 ± 296.9* [#]	2309.7 ± 396.9* ^{##}	3020.8 ± 568.9* ^{###} ¶
LVEDV (mL)	129.5 ± 34.1	124.2 ± 35.8	118.4 ± 34.5	115.4 ± 34.7	110.3 ± 39.1
LVESV (mL)	97.4 ± 29.3	84.3 ± 26.4*	74.8 ± 25.0* [#]	66.5 ± 24.2* ^{##}	56.7 ± 22.0* ^{###} ¶
LVSV (mL)	29.2 ± 11.0	36.6 ± 14.6	41.5 ± 13.3*	46.3 ± 12.6* ^{##}	52.2 ± 17.2* [#]
LVEF (%)	22.6 ± 6.0	29.5 ± 7.5*	35.2 ± 5.5* [#]	41.0 ± 5.9* ^{##}	48.1 ± 5.8* ^{###} ¶
RVEDV (mL)	94.2 ± 28.8	87.1 ± 29.5	82.0 ± 25.8*	80.6 ± 24.2*	82.7 ± 25.8
RVESV (mL)	80.0 ± 26.8	67.8 ± 26.8	59.2 ± 20.2*	55.5 ± 19.2* ^{##}	53.5 ± 21.7* [#]
RVEF (%)	15.8 ± 4.5	23.1 ± 7.5*	28.3 ± 4.5* [#]	32.1 ± 7.6* [#]	36.9 ± 9.8* ^{##}
CO _{Cb} (L/min)	3.1 ± 1.1	4.2 ± 1.8	4.9 ± 1.7*	5.8 ± 1.8* ^{##}	7.1 ± 2.6* ^{##}
CO _{Th} (L/min)	3.8 ± 2.0	6.0 ± 3.1*	7.4 ± 3.2*	9.4 ± 4.0* [#]	11.7 ± 5.2* [#]

N = 10 for all parameters except CO_{Th} and dP/dt_{max} (N = 8) for DCM dogs. Data are presented as mean ± SD. *P ≤ .05 vs baseline; [#]P ≤ .05 vs 2.5; ⁺P ≤ .05 vs 5; [¶]P ≤ .05 vs 10 $\mu\text{g}\cdot\text{kg}^{-1}\cdot\text{min}^{-1}$ (RM ANOVA, Tukey).

HR, heart rate; QRS interval, QRS complex duration; LVEDP, left ventricular end-diastolic pressure; dP/dt_{max}, maximum rate of LV pressure change; LVEDV and RVEDV, left and right end-diastolic volume; LVESV and RVESV, left and right end-systolic volume; LVSV, left ventricular stroke volume; LVEF and RVEF, left and right ventricular ejection fraction; CO_{Cb}, cardiac output by count-based method; CO_{Th}, cardiac output by thermodilution method.

Table 2. Dyssynchrony parameters at rest and during dobutamine-induced stress levels in DCM vs control dogs

Index	Dobutamine ($\mu\text{g}\cdot\text{kg}^{-1}\cdot\text{min}^{-1}$)				
	0	2.5	5	10	20
DCM					
LVCHI (%)	78.6 ± 10.9	84.5 ± 9.4	89.8 ± 5.2*	90.6 ± 5.4* [#]	92.4 ± 3.9* [#]
LV entropy	0.78 ± 0.09	0.71 ± 0.11	0.65 ± 0.09* [#]	0.63 ± 0.09* [#]	0.59 ± 0.08* ^{##}
LV Phase SD (°)	49.4 ± 14.8	41.0 ± 14.9	33.3 ± 10.6* [#]	31.9 ± 12.2* [#]	27.1 ± 10.7* [#]
RVLV delay (°)	-20.9 ± 21.1	-14.1 ± 13.9	-16.8 ± 10.2	-19.6 ± 10.7	-22.2 ± 11.5
RVLV delay (ms)	-33.3 ± 33.4	-20.3 ± 19.4	-23.4 ± 13.9	-25.8 ± 14.5	-27.6 ± 14.6
Control					
LVCHI (%)	96.4 ± 1.3	97.9 ± 0.6	98.7 ± 0.9*	98.6 ± 1.0	98.4 ± 1.2
LV entropy	0.52 ± 0.04	0.43 ± 0.03*	0.36 ± 0.09*	0.37 ± 0.10	0.38 ± 0.01
LV Phase SD (°)	25.4 ± 5.1	17.8 ± 6.4	12.8 ± 7.7	13.6 ± 8.0	15.0 ± 10.3
RVLV delay (°)	-6.3 ± 2.6	-10.7 ± 3.4	-19.3 ± 1.4*	-21.3 ± 3.6*	-21.6 ± 3.1*
RVLV delay (ms)	-13.9 ± 11.8	-17.2 ± 13.7	-17.8 ± 7.6	-23.8 ± 9.5	-23.5 ± 11.5

N = 10 for DCM dogs. N = 8 for Normal dogs. Data are presented as mean ± SD. *P ≤ .05 vs baseline; [#]P ≤ .05 vs 2.5; ⁺P ≤ .05 vs 5; [¶]P ≤ .05 vs 10 $\mu\text{g}\cdot\text{kg}^{-1}\cdot\text{min}^{-1}$ (RM ANOVA, Tukey).

LVCHI, LV contraction homogeneity index; RVLV delay, interventricular delay.

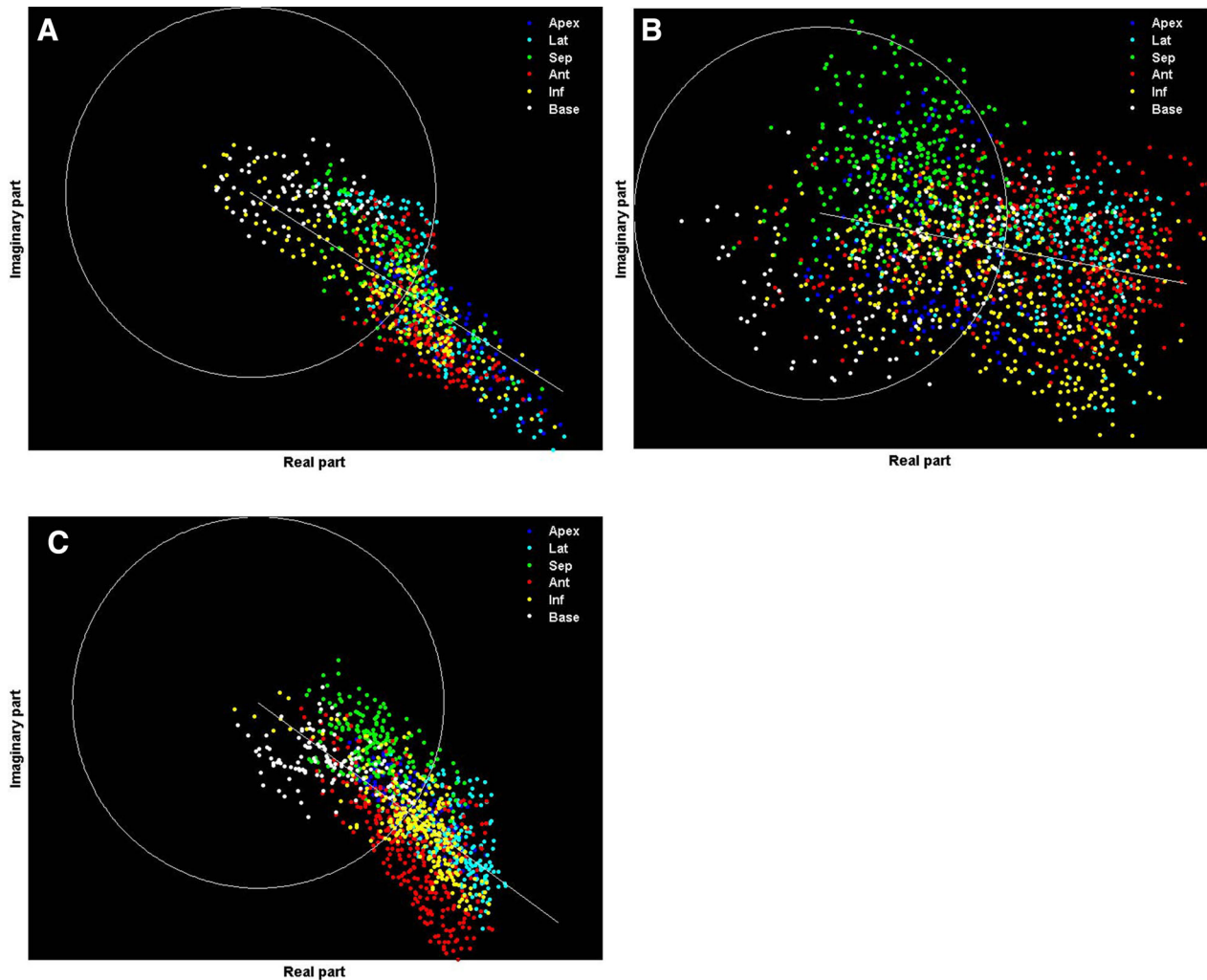


Figure 6. Illustration of count-based LV contraction phase in a control dog at baseline (A) and in a DCM dog at baseline (B) and at $20 \mu\text{g}\cdot\text{kg}^{-1}\cdot\text{min}^{-1}$ dobutamine level (C). Each of the 400 dots contains both amplitude and phase of an actual voxel within the LV ROI. They are expressed as a complex harmonic which contains both amplitude and phase ($Ae^{i\theta}$), represented in a polar coordinate system with a radius and angle that correspond to amplitude and phase, respectively. The *white circle* represents the average amplitude and the line is the direction of the average phase. In the normal subject, regional dots (complex harmonics) are homogeneously distributed around the mean phase and amplitude. However, in the DCM subject, the distribution of *dots* is almost uncoordinated around the *circle*. During the stress episodes, their distribution become more homogenous, potentially getting closer to the mean phase and amplitude, but still shows differences compared to the normal pattern.

RESULTS

Effects of Stress on Functional Parameters

Functional parameters at rest and during levels of dobutamine-induced stress in DCM dogs are shown in Table 1. D’Agostino-Pearson test confirmed that the distribution of the hemodynamic variables was not significantly different from a normal distribution ($P > .1$). The progressive dobutamine infusion resulted in a marked increase in heart rate, from

107.1 ± 10.5 bpm at rest to 134.7 ± 12.2 bpm for maximum level of pharmacological stress. Immediately after the initial pharmacological stimulation with a small amount of dobutamine, a significant increase in LVEF ($22.6\% \pm 6.0\%$ in baseline vs $29.5\% \pm 7.5\%$ in $2.5 \mu\text{g}\cdot\text{kg}^{-1}\cdot\text{min}^{-1}$; $P < .02$) was observed. Further significant differences were shown at higher levels ($P < .0001$). Interestingly, the same results were seen in RVEF ($P < .0001$). Also, a significant increasing trend was observed in the cardiac output by both radionuclide

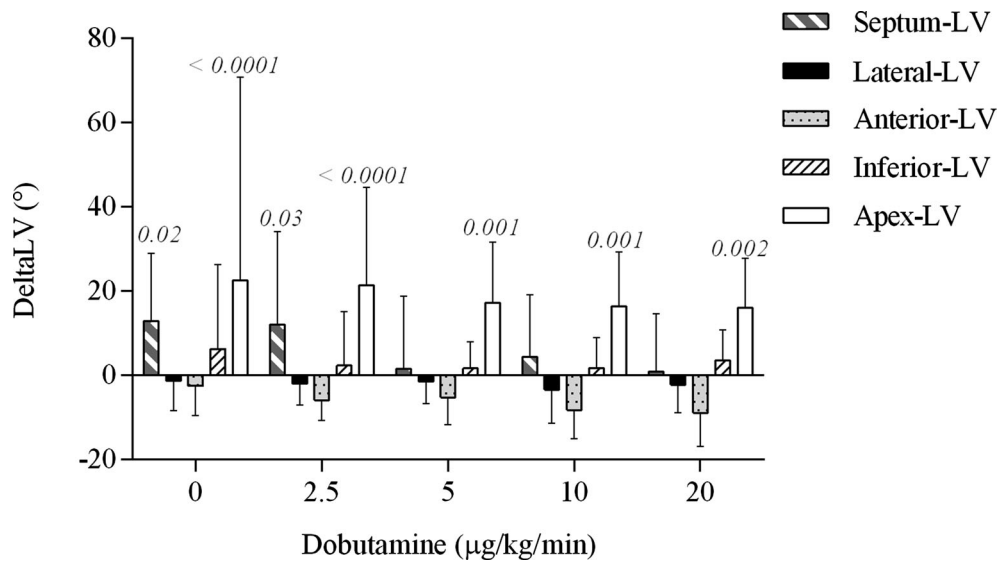


Figure 7. Left ventricular regional wall phase differences at baseline and at each dobutamine level. LV phase is the origin (zero) and each regional wall phase delay has been individually shown during the induction of dobutamine stress. Negative phases are earlier and positive values are more delayed sites of contraction. *P* values show the significant phase differences from zero.

and thermodilution methods with the increase of dobutamine doses ($P < .0001$), and methods indicated a good correlation in cardiac output measurements (Pearson's correlations at each dobutamine level > 0.7). Modulations of LV end-systolic and diastolic volumes (ESV, EDV) with increasing doses of dobutamine enhanced the stroke volume. Although the LV end-diastolic pressure (EDP) was still preserved in response to doses of dobutamine, volume alterations produced a constant progression in the maximum rate of rise of LV pressure (dP/dt_{max} ; $949.5 \pm 238.5 \text{ mmHg}\cdot\text{s}^{-1}$ at baseline vs $3020.8 \pm 568.9 \text{ mmHg}\cdot\text{s}^{-1}$ at $20 \mu\text{g}\cdot\text{kg}^{-1}\cdot\text{min}^{-1}$; $P < .0001$). QRS duration was almost constant and did not change significantly with the varying stress levels.

Effects of Stress on Intraventricular Dyssynchrony

Dyssynchrony parameters at rest and during dobutamine-induced stress levels in DCM vs control dogs are shown in Table 2. The D'Agostino-Pearson test confirmed that the distribution of the dyssynchrony variables did not significantly differ from a normal distribution ($P > .2$). All subjects revealed a significant amount of LV dyssynchrony at rest. However, dobutamine significantly increased the synchrony of contraction in all subjects. Figure 6A–C shows the count-based LV contraction phase of a control vs DCM dog at baseline and at maximum stress level. As has been shown, LV regions in a DCM subject contract according to different phases and amplitudes. Although

these uncoordinated contractions are substantially normalized at maximum stress level, they still show some differences when compared to the normal pattern. In the control group, a plateau was observed at the dobutamine level of $5 \mu\text{g}\cdot\text{kg}^{-1}\cdot\text{min}^{-1}$ for CHI and entropy values, meaning that $5 \mu\text{g}\cdot\text{kg}^{-1}\cdot\text{min}^{-1}$ dobutamine was an appropriate amount to generate maximum contraction efficiency in those subjects. In comparison, CHI showed a significant improvement from baseline to stress levels of $5 \mu\text{g}\cdot\text{kg}^{-1}\cdot\text{min}^{-1}$ dobutamine or greater ($P < .05$) in DCM subjects. Similar results were found for entropy and phase SD. Septal displacement was significantly out of phase with the LV (later than lateral wall at rest). However, it was normalized at peak dobutamine stress; this contrasts with the apex, which showed a significant difference relative to the LV phase and remained out of phase even at maximum stress ($P < .002$, Figure 7). An example of one DCM dog with reduced apex and septum contraction efficiency is shown in Figure 8.

Effects of Stress on Interventricular Dyssynchrony

Interventricular dyssynchrony was negative in all except one DCM subject at rest. A delay is defined as negative when the LV contracts earlier than the RV (Figure 9). Although a visual trend toward improvement of RVLV synchrony (approaching to zero) was observed with $2.5 \mu\text{g}\cdot\text{kg}^{-1}\cdot\text{min}^{-1}$ dobutamine, overall no significant change was seen between rest and the maximum stress level in this parameter, even when considering

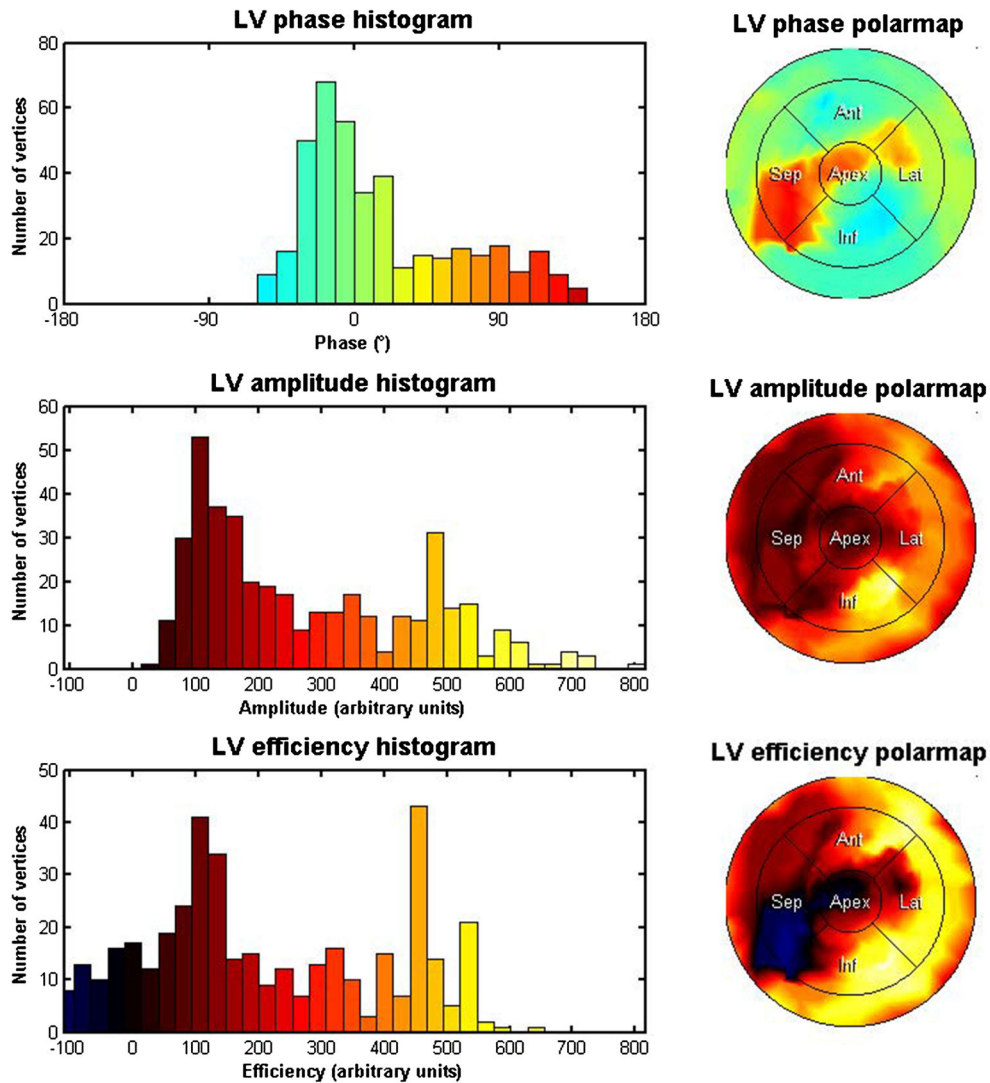


Figure 8. Illustration of phase, amplitude, and efficiency of all vertices in the LV of a DCM dog as an example in histogram and polar map displays. For this subject, the most important phase delays are located in the apex and septum. The apex shows approximately 90° phase delay (orange) compared to the average phase and lower amplitude (dark red) compared to the anterolateral or inferior regions as well as a zero efficiency (black). For the septum, the overall amplitude is lower than the rest of the ventricle, which is normal, since it is in the center of the ventricle and we measured the movements of the regions of the ventricle rather than the wall thickening. However, in this case, the septal delay is remarkable relative to other regions in the LV (red) which gives a negative efficiency or blue region in the efficiency polar map. For this example, the CHI has been reduced to 82% and the entropy increased to 73%.

absolute values $(-20.9 \pm 21.1^\circ (-33 \pm 33.4 \text{ ms})$ at baseline vs $-22.2 \pm 11.5^\circ (-27.6 \pm 14.6 \text{ ms})$ at $20 \mu\text{g}\cdot\text{kg}^{-1}\cdot\text{min}^{-1}$, $P < .25$; $25.0 \pm 15.4^\circ$ at baseline vs $22.2 \pm 11.5^\circ$ at $20 \mu\text{g}\cdot\text{kg}^{-1}\cdot\text{min}^{-1}$, in absolute values, $P < .08$; Table 2). In fact, as has been shown in Figure 9, there were individual differences in the magnitude and pattern of change in interventricular dyssynchrony during the various levels of dobutamine stress and it was hard to draw a certain direction of change in RVLV delay measurements.

Control vs DCM Group

Comparison of LV dyssynchrony and functional parameters between the DCM and control dogs at rest and at maximum stress level is shown in Table 3. In general, DCM dogs showed a depressed ventricular function (EF, dP/dt_{max}). Also, all intraventricular dyssynchrony indices in this cohort showed significant differences in comparison to the control subjects both at rest and under maximum stress levels (all lower than

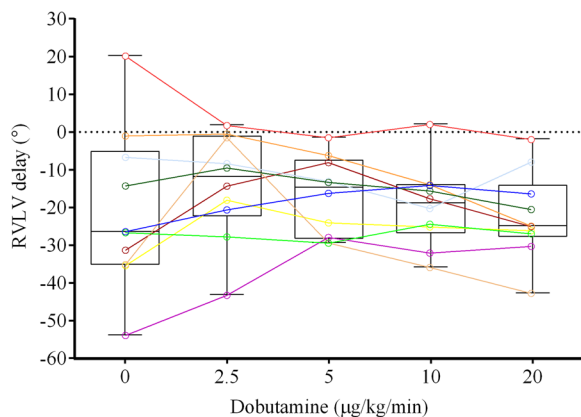


Figure 9. Interventricular mechanical dyssynchrony (RVLV delay) at rest and during different levels of dobutamine stress. For each dobutamine level, median and spread of phase delays are indicated in a box-and-whiskers plot. The *line* in the box marks the median and the hinges (limits of the box) indicate the range of observation with 5th–95th percentile. Whiskers show the minimum and maximum values in a column. Also, the trend of variations of RVLV delays during the dobutamine stress is shown for each dog in *color lines*.

normal values). In the DCM cohort, septal contraction always occurred later than LV lateral wall contraction. The introduction of cardiac stress did not change the pattern of mechanical contraction in the DCM cohort, which was always a lateral-to-septal (Figure 7), compared to LV contraction in the control group, where dobutamine-induced stress resulted in a septal-to-lateral pattern. There was no significant difference between the DCM and control subjects in interventricular mechanical dyssynchrony at rest ($P < .08$) and notably at maximum dobutamine stress ($P < .91$). In average, LV contraction preceded RV contraction in both groups at rest. Due to the increase in ventricular conduction speed, a progressive early LV contraction was apparent in subjects with normal cardiac contraction under dobutamine-induced stress. However, the interventricular synchrony was not hampered during the stress condition in these subjects. In comparison, individual differences in the magnitude and pattern of change in interventricular dyssynchrony precluded the existence of a statistically significant trend of change in this parameter during the various stages of dobutamine stress in the DCM cohort.

DISCUSSION

The range of difference in ventricular dyssynchrony parameters between rest and levels of stress has rarely been studied in cardiac failure subjects. The current study performed by GBPS showed that, even in close intervals, different levels of dobutamine stress could have a significant impact on ventricular function and

intraventricular dyssynchrony parameters in DCM subjects with narrow QRS complexes.

GBPS for Assessing Stress Dyssynchrony

In echocardiography, a few points in space and a few heartbeats are used to estimate either maximum temporal delay or standard deviation of delays over all LV segments. In contrast, GBPS uses several hundred data points in space and multiple data points in time that are taken from the analysis of a complete cardiac cycle which has been averaged over hundreds of cardiac cycles at the time of acquisition. Cross-correlation of the mean phase of all points, either regionally or globally, thus results in the direct measurement of mechanical dyssynchrony. GBPS is fully automated (in our case more than 90%) and provides highly reproducible dyssynchrony indices.¹⁰ In comparison, several different and complicated segmental analyses in echocardiography result in substantial errors and high inter- and intraobserver variability.⁸ Currently, GBPS plays a central role in the visual and quantitative characterization of LV dyssynchrony. However, it cannot replace GBPS, since GBPS can provide both inter- and intraventricular dyssynchrony data, especially in the presence of perfusion defects. Recently, GBPS has also been used to gain a better understanding of mechanical dyssynchrony and its efficacy in predicting the response to cardiac resynchronization therapy in HF patients^{20,21}.

Ventricular Dyssynchrony and Narrow QRS

The evidence found in the literature highlights the fact that QRS duration does not correlate with intraventricular dyssynchrony and has only a limited relationship with interventricular dyssynchrony.²² In a model with narrow QRS complex, we observed significant LV dyssynchrony and non-significant RVLV delay, which is in accordance with previous reports. In fact, QRS duration incorporates both right and LV activation, and one's delayed activation can be balanced by the other's rapid activation. In so doing, a normal QRS complex is preserved, in spite of a significant LV mechanical dyssynchrony. In the current study, while disparity in timing of ventricular mechanical contraction was obviously affected by levels of dobutamine stress, no specific alteration was observed in the duration of the QRS complex.

Dobutamine Stress and Ventricular Dyssynchrony

A limited number of echocardiographic studies have specifically addressed the effect of stress on

Table 3. Comparison of LV dyssynchrony and functional parameters between DCM and control dogs

	Rest			Maximum stress		
	Normal	DCM	<i>P</i> value	Normal	DCM	<i>P</i> value
HR (bpm)	112.1 ± 19.1	107.1 ± 10.5	.49	182.9 ± 15.6	134.7 ± 12.2	<.0001
QRS interval (ms)	76.5 ± 5.7	79.1 ± 10.2	.52	71.1 ± 9.0	78.2 ± 7.7	.09
LVEDV (mL)	52.2 ± 15.7	130.1 ± 34.3	<.0001	37.4 ± 14.5	110.3 ± 39.1	.0001
LVESV (mL)	30.9 ± 7.0	97.8 ± 29.4	<.0001	16.7 ± 2.8	56.7 ± 22.0	.0001
SV (mL)	25.8 ± 9.4	29.2 ± 11.0	.49	31.3 ± 12.3	52.2 ± 17.2	.01
LVEF (%)	49.5 ± 8.4	22.6 ± 6.0	<.0001	69.9 ± 12.4	48.1 ± 5.8	.0001
<i>dP/dt</i> _{max} (mmHg·s ⁻¹)	1588 ± 374	949.5 ± 238.5	.001	8004 ± 710	3020.8 ± 568.9	<.0001
CO_Cb (L/min)	2.8 ± 1.0	3.1 ± 1.1	.55	5.7 ± 2.2	7.1 ± 2.6	.24
CO_Th (L/min)	3.2 ± 1.3	3.8 ± 2.0	.47	7.9 ± 4.2	11.7 ± 5.2	.13
LVCHI (%)	96.4 ± 1.3	78.6 ± 10.9	.0003	98.4 ± 1.2	92.4 ± 3.9	.0008
LV entropy	0.52 ± 0.04	0.78 ± 0.09	.0001	0.38 ± 0.10	0.59 ± 0.08	.0002
LV phase SD (°)	25.4 ± 5.1	49.4 ± 14.8	.0005	15.0 ± 10.3	27.1 ± 10.7	.03
RVLV delay (°)	-6.3 ± 2.6	-20.9 ± 21.1	.08	-21.6 ± 3.1	-22.2 ± 11.5	.91
RVLV delay (ms)	-13.9 ± 11.8	-33.3 ± 33.4	.14	-23.5 ± 11.5	-27.6 ± 14.6	.53

N = 10 for all parameters except CO_Th and *dP/dt*_{max} (N = 8) in DCM dogs. N = 8 for all except *dP/dt*_{max} at 20 μg·kg⁻¹·min⁻¹ dobutamine (N = 6) in control dogs. Data are presented as mean ± SD.

HR, heart rate; QRS interval, QRS complex duration; LVEDV and LVESV, left ventricular end-diastolic and systolic volume; SV, stroke volume; LVEF, left ventricular ejection fraction; *dP/dt*_{max}, maximum rate of LV pressure change; CO_Cb, cardiac output by count-based method; CO_Th, cardiac output by thermodilution method; LVCHI, LV contraction homogeneity index; RVLV delay, inter-ventricular delay.

mechanical dyssynchrony in DCM patients with narrow QRS complexes.⁴⁻⁷ In these studies, three distinct groups of patients could be identified based on a specific dyssynchrony parameter: the first group showed no difference between rest and stress, the second showed an induced dyssynchrony when going from rest to stress, and the last showed a normalized dyssynchrony when going from rest to stress. The reason the patients manifested such variable responses to exercise or dobutamine stress is not clear. What we observed in our study was the same response from all DCM subjects, with exactly the same induced pathology, in terms of LV intraventricular dyssynchrony parameters at stress. Based on our regional analysis, improvement of LV mechanical dyssynchrony at stress was attributable to the early contraction of previously delayed-contracting regions that were mostly seen in the LV apex and septum. Our observations concur with the evidence collected by Somsen et al, according to whom the septal wall is the typical site of dyskinesia and reduced contractility in patients with DCM,²³ as well as with a recent canine study performed by strain echocardiography which showed a larger decrease on strains of apical segments in DCM dogs.¹² Under induced stress, only the late septal contraction was normalized. The absence of any protection from the mitral annulus and papillary muscles in the apex could be the cause of severe

tachycardia-induced effects in this region rather than on other walls at the time of evolution of LVDCM.¹²

Intermediate levels of dobutamine stress caused significant changes in homogeneity of contraction and ventricular function in the DCM cohort. Applied LV dyssynchrony indices allowed for a clear distinction between those changes during the various stages of stress. Even in control subjects, CHI and entropy sensitivity were promising in specifying the dyssynchrony variations during the stress condition. This observation concurred with what was previously seen in wall thickening-derived CHI and entropy when these were used to evaluate stress dyssynchrony in a control group.²⁴ However, because phase values were well peaked in control subjects, phase SD could not show the small variances during the induction of dobutamine stress. Overall, our LV dyssynchrony parameters did not contradict, but rather complemented, each other in the stress analysis, in contrast to the previously seen discordance between the parameters of dyssynchrony measured by stress echocardiography in HF patients.⁵

In the current study, interventricular mechanical dyssynchrony was found to be insignificant in DCM subjects compared to their normal counterparts. A similar observation was made by another group who showed that interventricular mechanical dyssynchrony is less frequently noted in HF patients with narrow QRS

complexes.²⁵ The main point here is the variability of the baseline direction of contraction (1 out of 10 subjects with positive RVLV delay), also seen in the control group (2 out of 8 dogs showed positive RVLV delays).¹³ Moreover, there was an individual difference in the magnitude and pattern of change in RVLV delays during the dobutamine stress that was also seen in the control group. We could not explain the reason of such variability in RVLV delays between individuals, which might be related to individual cardiac mechanical characteristics.

LIMITATIONS

The current study was performed in dogs; consequently, even though the applied methodology may seem transferable, our findings are not directly transferable to humans. The number of animals was limited in this study. The inadequate number of subjects, as well as inter-animal variability in RVLV delays, precluded any definitive conclusion about the effects of maximum stress in interventricular dyssynchrony. Due to the limited spatial resolution of the SPECT system, we relied on a count-based analysis to quantify dyssynchrony indices, an alternative superior to volume-based measurements, since it is more reproducible and accurate. The apparent ventricular movement was actually the movement of blood-endocardial interface. Consequently, global cardiac motion was also present during ventricular systole along with myocardial contraction, which made it impossible to distinguish the real endocardial movements. Although global cardiac motion was likely to be small in LV, it could severely affect the RV due to its geometrical shape. For this reason, we did not measure the RV intraventricular dyssynchrony indices. The best scenario for RV was probably to be in synchrony with the LV which is thicker and more concentric (RVLV delay). Finally, differences in synchrony between rest and stress episodes could be interpreted as being due to a better image resolution and count statistics caused by higher heart rates rather than by the intrinsic physiologic effects of stress. This hypothesis was previously evaluated by positron emission tomography and results revealed that count statistics are not responsible for the difference in dyssynchrony indices at stress.²⁶ However, this might not be as clear-cut in the case of SPECT images when image quality and count statistics are different.

NEW KNOWLEDGE GAINED

Stress ventricular dyssynchrony analysis can be assessed in a straightforward and fully automated manner by phase analysis of GBPS imaging. Different

levels of dobutamine stress, even in close intervals, can have a significant impact on intraventricular dyssynchrony parameters in DCM subjects with narrow QRS complexes. The changing trends are mostly seen as going toward the perfection of synchrony. The dyssynchrony indices of CHI, entropy, and phase SD have the same sensitivity to distinguish between various stress levels in DCM subjects.

CONCLUSION

In this study with a non-ischemic DCM model with a narrow QRS complex, GBPS could identify the extent and pattern of ventricular contraction dyssynchrony at rest and during dobutamine stress levels. Different levels of functional stress, even in close intervals, made significant positive changes in hemodynamic and intraventricular dyssynchrony parameters. Since evidence of stress-induced mechanical dyssynchrony may be helpful in predicting the response to cardiac resynchronization therapy, further research is warranted to assess whether lower ventricular mechanical dyssynchrony indices induced by stress and measured by GBPS have the ability to predict the response to resynchronization therapy.

Acknowledgments

This study was conducted with the collaboration of the Electrophysiology Service of the Montreal Heart Institute. We wish to thank Marc-Antoine Gillis, Evelyn Landry, Marie-Pierre Mathieu, and Sophie Marcil for their expert technical assistance.

Disclosure

The authors declare that they have no conflict of interest.

References

1. Kass DA. An epidemic of dyssynchrony: But what does it mean? *J Am Coll Cardiol* 2008;51:12-7.
2. Matsumoto K, Tanaka H, Tatsumi K, Kaneko A, Tsuji T, Ryo K, et al. Regional heterogeneity of systolic dysfunction is associated with ventricular dyssynchrony in patients with idiopathic dilated cardiomyopathy and narrow QRS complex. *Echocardiography* 2012;29:1201-10.
3. Ghio S, Constantin C, Klersy C, Serio A, Fontana A, Campana C, et al. Interventricular and intraventricular dyssynchrony are common in heart failure patients, regardless of QRS duration. *Eur Heart J* 2004;25:571-8.
4. D'andrea A, Mele D, Nistri S, Riegler L, Galderisi M, Losi MA, et al. The prognostic impact of dynamic ventricular dyssynchrony in patients with idiopathic dilated cardiomyopathy and narrow QRS. *Eur Heart J Cardiovasc Imaging* 2013;14:183-9.
5. Lafitte S, Bordachar P, Lafitte M, Garrigue S, Reuter S, Reant P, et al. Dynamic ventricular dyssynchrony: An exercise-echocardiography study. *J Am Coll Cardiol* 2006;47:2253-9.

6. Chattopadhyay S, Alamgir MF, Nikitin NP, Fraser AG, Clark AL, Cleland JG. The effect of pharmacological stress on intraventricular dyssynchrony in left ventricular systolic dysfunction. *Eur J Heart Fail* 2008;10:412-20.
7. Yagishita-Tagawa Y, Abe Y, Arai K, Yagishita D, Takagi A, Ashihara K, et al. Low-dose dobutamine induces left ventricular mechanical dyssynchrony in patients with dilated cardiomyopathy and a narrow QRS: A study using real-time three-dimensional echocardiography. *J Cardiol* 2013;61:275-80.
8. Chung ES, Leon AR, Tavazzi L, Sun JP, Nihoyannopoulos P, Merlino J, et al. Results of the predictors of response to CRT (Prospect) trial. *Circulation* 2008;117:2608-16.
9. Lancellotti P, Moonen M. Left ventricular dyssynchrony: A dynamic condition. *Heart Fail Rev* 2012;17:747-53.
10. Trimble MA, Velazquez EJ, Adams GL, Honeycutt EF, Pagnanelli RA, Barnhart HX, et al. Repeatability and reproducibility of phase analysis of gated single-photon emission computed tomography myocardial perfusion imaging used to quantify cardiac dyssynchrony. *Nucl Med Commun* 2008;29:374.
11. Lalonde M, Birnie D, Ruddy TD, Wassenaar RW. SPECT blood pool phase analysis can accurately and reproducibly quantify mechanical dyssynchrony. *J Nucl Cardiol* 2010;17:803-10.
12. Kusunose K, Zhang Y, Mazgalev TN, Thomas JD, Popovic ZB. Left ventricular strain distribution in healthy dogs and in dogs with tachycardia-induced dilated cardiomyopathy. *Cardiovasc Ultrasound* 2013;11:43.
13. Harel F, Finnerty V, Gregoire J, Salimian S, Thibault B. Effects of dobutamine stress on cardiac contraction synchronism in a canine model. *Physiol Meas* 2013;34:1387-97.
14. Ganz W, Donoso R, Marcus HS, Forrester JS, Swan HJ. A new technique for measurement of cardiac output by thermodilution in man. *Am J Cardiol* 1971;27:392-6.
15. Harel F, Finnerty V, Ngo Q, Gregoire J, Khairy P, Thibault B. SPECT versus planar gated blood pool imaging for left ventricular evaluation. *J Nucl Cardiol* 2007;14:544-9.
16. Harel F, Finnerty V, Grégoire J, Thibault B, Marcotte F, Ugolini P, et al. Gated blood-pool SPECT versus cardiac magnetic resonance imaging for the assessment of left ventricular volumes and ejection fraction. *J Nucl Cardiol* 2010;17:427-34.
17. Harel F, Finnerty V, Grégoire J, Thibault B, Khairy P. Comparison of left ventricular contraction homogeneity index using SPECT gated blood pool imaging and planar phase analysis. *J Nucl Cardiol* 2008;15:80-5.
18. O'Connell JW, Schreck C, Moles M, Badwar N, DeMarco T, Olgin J, et al. A unique method by which to quantitate synchrony with equilibrium radionuclide angiography. *J Nucl Cardiol* 2005;12:441-50.
19. Wassenaar R, O'Connor D, Dej B, Ruddy TD, Birnie D. Optimization and validation of radionuclide angiography phase analysis parameters for quantification of mechanical dyssynchrony. *J Nucl Cardiol* 2009;16:895-903.
20. Lalonde M, Birnie D, Ruddy TD, Beanlands RS, Wassenaar R, Wells RG. SPECT gated blood pool phase analysis of lateral wall motion for prediction of CRT response. *Int J Cardiovasc Imaging* 2014;30:559-69.
21. Lalonde M, Wells RG, Birnie D, Ruddy TD, Wassenaar R. Development and optimization of SPECT gated blood pool cluster analysis for the prediction of CRT outcome. *Med Phys* 2014;41:072506.
22. Hawkins NM, Petrie MC, MacDonald MR, Hogg KJ, McMurray JJ. Selecting patients for cardiac resynchronization therapy: Electrical or mechanical dyssynchrony? *Eur Heart J* 2006;27:1270-81.
23. Somsen GA, Verberne HJ, Burri H, Ratib O, Righetti A. Ventricular mechanical dyssynchrony and resynchronization therapy in heart failure: A new indication for Fourier analysis of gated blood-pool radionuclide ventriculography. *Nucl Med Commun* 2006;27:105-12.
24. Salimian S, Thibault B, Finnerty V, Grégoire J, Harel F. The effects of dobutamine stress on cardiac mechanical synchrony determined by phase analysis of gated SPECT myocardial perfusion imaging in a canine model. *J Nucl Cardiol* 2014;21:375-83.
25. van Bommel RJ, Tanaka H, Delgado V, Bertini M, Borleffs CJW, Marsan NA, et al. Association of intraventricular mechanical dyssynchrony with response to cardiac resynchronization therapy in heart failure patients with a narrow QRS complex. *Eur Heart J* 2010;31:3054-62.
26. AlJaroudi W, Alraies MC, DiFilippo F, Brunken RC, Cerqueira MD, Jaber WA. Effect of stress testing on left ventricular mechanical synchrony by phase analysis of gated positron emission tomography in patients with normal myocardial perfusion. *Eur J Nucl Med Mol Imaging* 2012;39:665-72.